Molecular Crystals and Liquid Crystals

Publication details, including instructions for authors and subscription information:
http://www.tandfonline.com/loi/gmcl20

Simulations of the Elastic Bent-Core Molecules

W. Józefowicz [a] & L. Longa [a]

[a] Marian Smoluchowski Institute of Physics, Department of Statistical Physics and Mark Kac Complex Systems Research Center, Jagellonian University, Kraków, Poland

Version of record first published: 22 Sep 2010

To cite this article: W. Józefowicz & L. Longa (2007): Simulations of the Elastic Bent-Core Molecules, Molecular Crystals and Liquid Crystals, 478:1, 115/[871]-123/[879]

To link to this article: http://dx.doi.org/10.1080/15421400701738586

Mol. Cryst. Liq. Cryst., Vol. 478, pp. 115/[871]–123/[879], 2007

ISSN: 1542-1406 print/1563-5287 online
DOI: 10.1080/15421400701738586

Taylor & Francis
Taylor & Francis Group

Simulations of the Elastic Bent-Core Molecules

W. Józefowicz
L. Longa
Marian Smoluchowski Institute of Physics, Department of Statistical Physics and Mark Kac Complex Systems Research Center, Jagellonian University, Kraków, Poland

An influence of thermal fluctuations in opening angle was studied for a model of bent-core molecules using MC NPT computer simulation. The elastic bent-core shape was modeled by joining two Gay-Berne particles through the harmonic bond. Results for two stiff bananas with fixed opening angles of $\phi = 120^\circ$ and $\phi = 140^\circ$ were compared with their elastic counterparts. For all systems studied we found that with the varying opening angle the melting point moves towards lower temperatures. We did not discover any new phase as compared to the stiff cases.

Keywords: bent-core; MC simulations; variable opening angle

I. INTRODUCTION

The achiral banana-shaped molecules show many interesting properties among which is the formation of the biaxial nematics [1,2] and of the local twisted configurations [3,4]. Although these structures were found to exist in real experiments the essential molecular features responsible for their stability still remain unclear. One of the tools with which to study a connection between intermolecular interactions and structure formation are computer simulations. Using Monte Carlo (MC) and molecular dynamics (MD) we can seek for the simplest

This work was supported by Grant N202 169 31/3455 of Polish Ministry of Science and Higher Education, and by the EC Marie Curie Actions 'Transfer of Knowledge', project *COCOS* (contract MTKD-CT-2004-517186). We also gratefully acknowledge the computing grant G27-8 towards the use of the ICM (University of Warsaw) computers.

Address correspondence to Wojciech Józefowicz, Marian Smoluchowski Institute of Physics, Department of Statistical Physics and Mark Kac Complex Systems Research Center, Instytut Fizyki UJ, ul. Reymonta 4, Krakow, 30-059, Poland. E-mail: wjozefow@th.if.uj.edu.pl

molecular models revealing given macroscopic behavior. Recently, a variety of model bent-core systems have been proposed [5–8], neither of them, however, reveals the biaxial nematic nor provides convincing proof of the existence of the twisted chiral structures.

In this work we focus on the model bent-core molecules allowing for fluctuations in the opening angle. The molecule is built out of two Gay-Berne particles connected by angle-dependent harmonic interactions. The motivation for such approach comes from expectation that elastic arms of the bent-core could destabilize crystalline phases in favour of nematic ones.

II. MODEL SYSTEM

A banana-shaped Gay-Berne molecule is defined by linking two prolate Gay-Berne particles, a and b, Figure 1. The molecule is parameterized by two internal coordinates: (i) the bending angle ϕ between the unit vectors $\hat{\mathbf{u}}_a$ and $\hat{\mathbf{u}}_b$ placed along banana arms ($0^0 < \phi < 180^\circ$) and (ii) the intramolecular distance $r_{ab} = |\mathbf{r}_{ab}| = |\mathbf{r}_b - \mathbf{r}_a|$, where $\mathbf{r}_a$ and $\mathbf{r}_b$ are the centers of the two Gay-Berne particles. The angle ϕ is free to vary about fixed ϕ_0, $r_{ab} = \sqrt{2c^2(1-\cos\phi)}$ and c is the shift of the centers of both GB particles along the banana arms.

In addition, we introduce a molecule-fixed coordinate system with axes $\{x^*_\mu,\ \mu = 1,2,3\}$, where x^*_3 is taken parallel to the intramolecular vector $\mathbf{r}_{ab}$, x^*_2 is placed along $\hat{\mathbf{u}}_a + \hat{\mathbf{u}}_b$, and finally x^*_1 is perpendicular to both x^*_2 and x^*_3. The axes $\{x^*_1, x^*_2, x^*_3\}$ form a right-handed Cartesian coordinate system. Details of the parametrization are shown in Figure 1.

The intermolecular interactions between pair of molecules i and j, separated by an intermolecular vector $\mathbf{R}_{ij} = \frac{1}{2}[(\mathbf{r}_a^{(j)} + \mathbf{r}_b^{(j)}) - (\mathbf{r}_a^{(i)} + \mathbf{r}_b^{(i)})]$

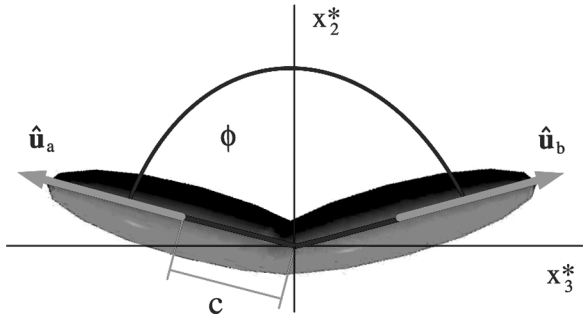

FIGURE 1 Model of bent-core molecule composed of two Gay-Berne particles.

are given by

$$U(\Omega_i, \Omega_j, \mathbf{R}_{ij}) = \sum_{\alpha=a,b} \sum_{\beta=a,b} U_{GB}(\hat{\mathbf{u}}_\alpha^{(i)}, \hat{\mathbf{u}}_\beta^{(j)}, \mathbf{r}_{\alpha\beta}^{(i,j)}), \tag{1}$$

where Ω_i of the molecule i stands for the Euler angles $\alpha_i, \beta_i, \gamma_i$ between the space-fixed coordinate system x'_μ and the molecule-fixed system $x^*_{\mu,i}$ ($\mu = 1, 2, 3$); $\mathbf{r}_{\alpha\beta}^{(i,j)} = \mathbf{r}_\beta^{(j)} - \mathbf{r}_\alpha^{(i)}$ denotes the intermolecular vector between the center of part α of the molecule i and the center of part β of the molecule j ($\alpha, \beta = a, b$).

The interaction potential U_{GB} between the parts α, β of the molecules i and j, respectively, is of the Gay-Berne form [9]

$$U_{GB}(\hat{\mathbf{u}}_\alpha^{(i)}, \hat{\mathbf{u}}_\beta^{(j)}, \mathbf{r}_{\alpha\beta}^{(i,j)}) = 4\,\epsilon(\hat{\mathbf{u}}_\alpha^{(i)}, \hat{\mathbf{u}}_\beta^{(j)}, \hat{\mathbf{r}}_{\alpha\beta}^{(i,j)}) \left[\left(\frac{\sigma_0}{r_{\alpha\beta}^{(i,j)} - \sigma(\hat{\mathbf{u}}_\alpha^{(i)}, \hat{\mathbf{u}}_\beta^{(j)}, \hat{\mathbf{r}}_{\alpha\beta}^{(i,j)}) + \sigma_0} \right)^{12} - \left(\frac{\sigma_0}{r_{\alpha\beta}^{(i,j)} - \sigma(\hat{\mathbf{u}}_\alpha^{(i)}, \hat{\mathbf{u}}_\beta^{(j)}, \hat{\mathbf{r}}_{\alpha\beta}^{(i,j)}) + \sigma_0} \right)^{6} \right], \tag{2}$$

where $\hat{\mathbf{r}}_{\alpha\beta}^{(i,j)}$ denotes the unit vector parallel to $\mathbf{r}_{\alpha\beta}^{(i,j)}$ and $r_{\alpha\beta}^{(i,j)} = |\mathbf{r}_{\alpha\beta}^{(i,j)}|$. Functions $\epsilon(\hat{\mathbf{u}}_\alpha^{(i)}, \hat{\mathbf{u}}_\beta^{(j)}, \hat{\mathbf{r}}_{\alpha\beta}^{(i,j)})$ and $\sigma(\hat{\mathbf{u}}_\alpha^{(i)}, \hat{\mathbf{u}}_\beta^{(j)}, \hat{\mathbf{r}}_{\alpha\beta}^{i,j})$ depend on four parameters κ, κ', μ and ν. The explicit expressions for these functions are given in [9].

Each molecule i is allowed to vary its bending angle ϕ_i about ϕ_0 with a harmonic contribution to the potential energy

$$U_i^{harm}(\phi_i) = k(\phi_i - \phi_0)^2, \tag{3}$$

where k is the harmonic constant.

III. COMPUTATIONAL DETAILS

For the model defined in the previous section we arbitrarily chose $c = 1.7\sigma_0$, which corresponds to smooth molecular shape for all opening angles in the range studied (Fig. 8). The Gay-Berne sites were parametrized with the following set of constants: $\kappa = 4$, $\kappa' = 5$, $\mu = 1$ and $\nu = 2$ [5]. We studied four different combinations of the remaining parameters: (a) $k = \infty, \phi_0 = 120°$; (b) $k = \infty, \phi_0 = 140°$ for rigid molecules and (c) $k = 25, \phi_0 = 120°$; (d) $k = 25, \phi_0 = 140°$ for their elastic counterparts.

Monte Carlo simulations were performed in a rectangular box at constant number of particles N, constant pressure P and constant

temperature T (NPT ensemble). The periodic boundary conditions and the nearest image convention were taken regard of. For elastic molecules, the sequence of configurational states was generated in agreement with the probability density:

$$f(\Gamma,\Omega,\Phi)=\Pi_{i=1}^{N}\sqrt{\left(1+3\cos^2\frac{\phi_i}{2}\right)\left(1-\cos^2\frac{\phi_i}{2}\right)\cos^2\frac{\phi_i}{2}\left(4-3\cos^2\frac{\phi_i}{2}\right)}\times\exp(-(U_{total}(\Gamma,\Omega,\Phi)+PV-NT\ln V)/T)/Z'_{NPT}, \quad (4)$$

where Γ,Ω,Φ denote respectively positions, orientations and opening angles of all particles, V is the volume of the system, U_{total} represents total potential energy and Z'_{NPT} denotes normalization factor (Boltzmann constant, not present in Equation (4), is included into definition of the dimensionless temperature T). The formula for the probability density (4) is essentially the same as one used in [10]. The only difference is the nontrivial square root contribution coming from the integration over momenta of the kinetic energy. For stiff molecules this part is a constant and, hence, can be merged with Z'_{NPT}. Note that all variables used in this paper were rendered dimensionless by using reduced units (*see e.g.*, [5]).

Simulations were carried out for $N=1000$, under the pressure $P=3$ and with spherical cutoff for the GB potential at the distance $\mathbf{r}_{\alpha\beta}^{(i,j)}=5.0$. The value for pressure was taken from Memmer's paper, devoted to simulations of stiff bent-core molecules [5].

The MC cycle of our simulations consisted of probing a new configuration for each particle followed by the change of a randomly chosen edge of the box. Within this routine a new configuration for each particle was generated by a random move of its center of mass, a random rotation about randomly chosen axis out of $\hat{\mathbf{x}}'_1,\ \hat{\mathbf{x}}'_2,\ \hat{\mathbf{x}}'_3$, a flip of the steric dipole, and a random change of the opening angle.

We started our simulations at low temperature. As an initial configuration we chose the hexagonal crystal with ferroelectric order of steric dipoles within a layer and antiferroelectric order between layers (Fig. 6(b)). We decided to use this kind of initial configuration for it appeared stable at low temperatures in the system of stiff particles simulated by Memmer [5].

The equilibration took between 500 kilocycles and 1000 kc after which the data for structure analysis were collected once per 20 cycles for a 20 kc production run. Simulations started at the temperature $T=0.5$, which was next increased in step of $\Delta T=0.5$. In the vicinity of phase transitions the step was reduced to 0.1.

IV. ORDER PARAMETERS AND CORRELATION FUNCTIONS

In order to characterize the long-range orientational order of the molecules, second rank order parameters $\langle P_2\rangle^{(\mu)}$ were calculated. They are given by the largest eigenvalue of the corresponding alignment tensors

$$S_{\alpha\beta}^{(\mu)} = \left\langle \frac{1}{N}\sum_{j=1}^{N}\left[\frac{3}{2}\hat{\mathbf{x}}_{j\alpha}^{(\mu)}\hat{\mathbf{x}}_{j\beta}^{(\mu)} - \frac{1}{2}\delta_{\alpha\beta}\right]\right\rangle, \tag{5}$$

where $\alpha,\beta = x,y,z$; $\hat{\mathbf{x}}_j^{(\mu)}$ denotes a unit vector along the molecule-fixed axis $x_{\mu,j}^*$ $(\mu = 1,2,3)$ of the molecule j. These eigenvalues read

$$\langle P_2\rangle^{(\mu)} = \left\langle \frac{1}{2}(3\cos^2\beta_j^{(\mu)} - 1)\right\rangle, \tag{6}$$

where $\beta_j^{(\mu)}$ is the angle between the molecule-fixed axis $x_{\mu,j}^*$ and director $\hat{\mathbf{n}}_\mu$, which is given by the eigenvector corresponding to the largest eigenvalue $\langle P_2\rangle^{(\mu)}$ of $S_{\alpha\beta}^{(\mu)}$.

Assuming $\hat{\mathbf{n}}_3$ to be parallel to x_3' the positional order along the director $\hat{\mathbf{n}}_3$ can be quantified in terms of the translational order parameter

$$\tau_1 = |\langle \exp(-2\pi i z)/d)\rangle|, \tag{7}$$

where z is the reduced coordinate along the director and d is the smectic layer spacing. Initially unknown layer spacing is adjusted by maximizing the translational order parameter with respect to d. Clearly, for the ideal nematic liquid $\tau_1 = 0$ while for the ideal smectic A phase $\tau_1 = 1$.

With the order parameters just defined we can distinguish between isotropic-, nematic- and layered structures. To probe the ordering within the layers we used the transversal pair distribution function $g_\perp^{(2)}(r_\perp)$:

$$g_\perp^{(2)}(r_\perp) = \frac{V}{4\pi r_\perp D N^2}\left\langle \sum_i\sum_{j\neq i}\delta(r_\perp - |\mathbf{r}_i - \mathbf{r}_j|_\perp)\Theta(D - |z_i - z_j|)\right\rangle, \tag{8}$$

where $r_\perp$ is the separation between the centers of mass of the molecules, projected onto a plane orthogonal to $\hat{\mathbf{n}}_3$, D is a parameter set to 1.0 and Θ is the Heaviside function.

V. RESULTS AND DISCUSSION

We start our discussion by looking at the results obtained for $k = \infty$ and $\phi_0 = 120^\circ$. For $T \leq 3.5$ the structure of phases found was consistent with the hexagonal, antiferroelectric and biaxial crystalline ordering

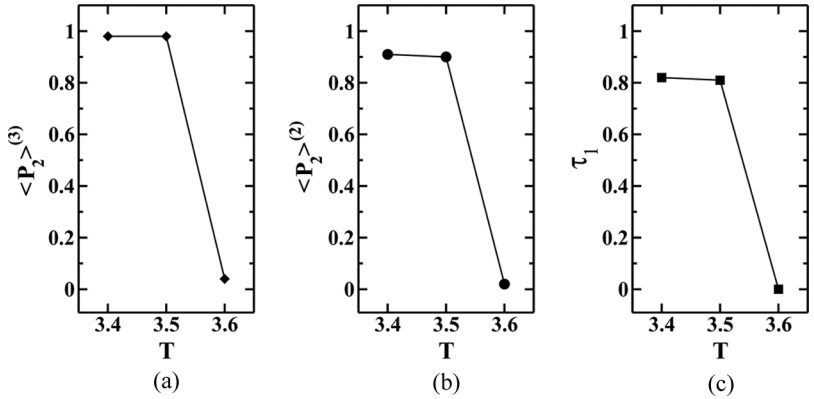

FIGURE 2 Temperature dependence of the order parameters: (a) $\langle P_2 \rangle^{(3)}$; (b) $\langle P_2 \rangle^{(2)}$ and (c) τ_1 for $k = \infty$ (rigid model) and $\phi_0 = 120^\circ$. Between temperatures $T = 3.5$ and 3.6 there is a phase transition from biaxial, antiferroelectric, hexagonal crystal into isotropic liquid.

(Figs. 2, 3), which was used as a starting configuration. Owing small system size we were unable to distinguish in our simulation between hexagonal crystal and hexatic smectic. Hence all phases with considerable hexagonal order within layers were (and are here) referred to as crystals. Highly ordered phase found for $T = 3.5$ has melted directly into isotropic liquid for $T = 3.6$ (Fig. 2). The same kind of behavior was observed for $k = 25$ and $\phi_0 = 120^\circ$ but the transition took place at lower temperature $T = 3.3$ (Fig. 4). For this temperature the

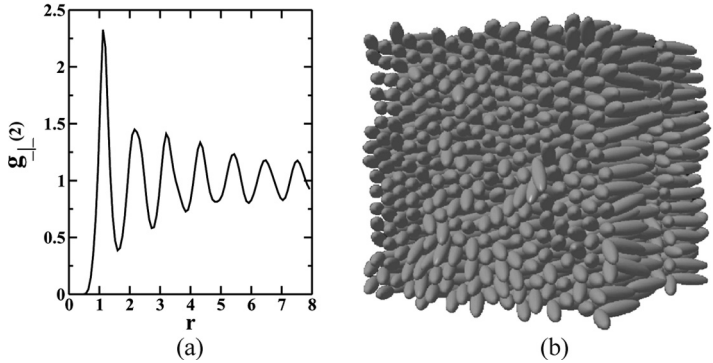

FIGURE 3 (a) Function $g_\perp^{(2)}$ describing layers' structure of the crystal obtained for $k = \infty$ (rigid model), $\phi_0 = 120^\circ$, and $T = 3.5$; (b) snapshot showing hexagonal-like long-range order of this phase.

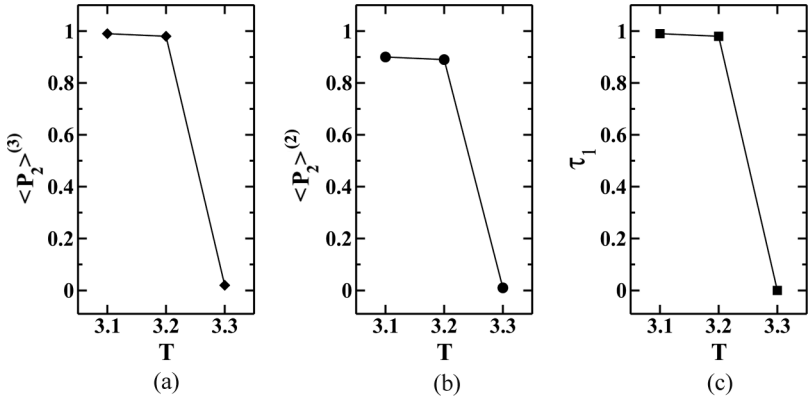

FIGURE 4 Temperature dependence of the order parameters: (a) $\langle P_2 \rangle^{(3)}$; (b) $\langle P_2 \rangle^{(2)}$ and (c) τ_1 for $k = 25$ and $\phi_0 = 120°$. Between temperatures $T = 3.2$ and 3.3 there is a phase transition from biaxial, antiferroelectric, hexagonal crystal into isotropic liquid.

histogram of the opening angles shows that the shape polydispersivity in the isotropic phase is of the order of 40° (Fig. 8(a)).

For $k = \infty$ and $\phi_0 = 140°$ the initial state has melted into a nematic phase. The evidence is shown in Figures 5, 6(a): the $S^{(2)}_{\alpha\beta}$ tensor has one negative eigenvalue for the eigenvector $\hat{\mathbf{n}}_3$ and two almost identical positive eigenvalues, denoted $\langle P_2 \rangle^{(2)}$ (Fig. 5). That is the steric dipoles

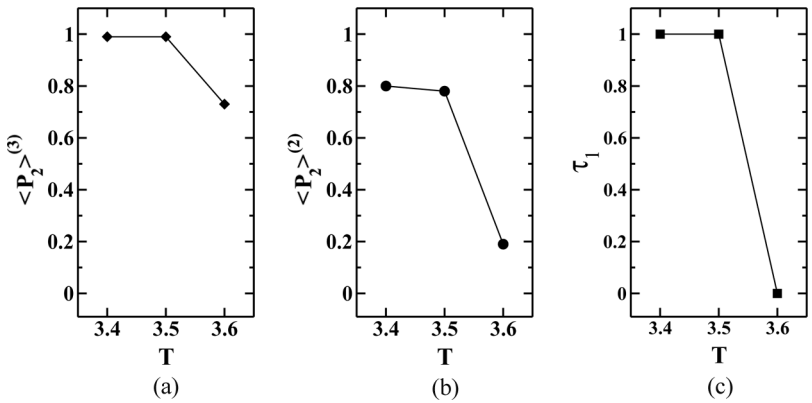

FIGURE 5 Temperature dependence of the order parameters: (a) $\langle P_2 \rangle^{(3)}$; (b) $\langle P_2 \rangle^{(2)}$ and (c) τ_1 for $k = \infty$ (rigid model) and $\phi_0 = 140°$. Between temperatures $T = 3.5$ and 3.6 there is a phase transition from biaxial, antiferroelectric, hexagonal crystal into uniaxial nematic.

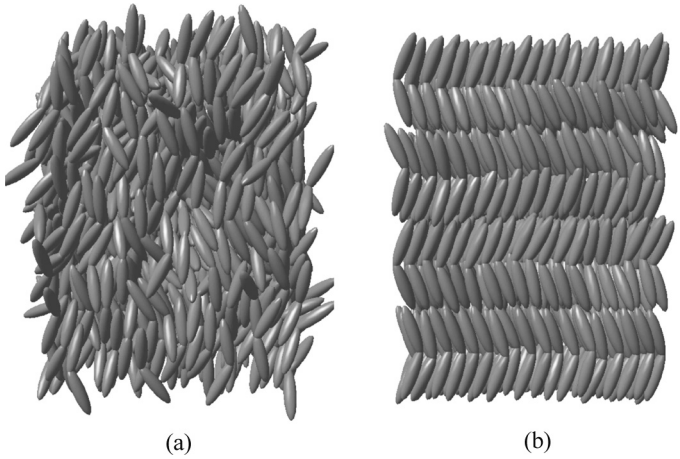

FIGURE 6 (a) Snapshot of nematic phase obtained for $T = 3.6$, $k = \infty$ (rigid model) and $\phi_0 = 140°$; (b) snapshot of biaxial, hexagonal, antiferroelectric crystalline structure obtained for $T = 3.5$, $k = \infty$ and $\phi_0 = 140°$.

of the molecules are, on the average, perpendicular to $\hat{\mathbf{n}}_3$ and uniaxially distributed about $\hat{\mathbf{n}}_3$. Hence the phase was the uniaxial nematic. In our simulations we were particulary interested in checking whether biaxial nematic can be made stable in our system. Unfortunately, for the parameters studied, our results were negative in this respect.

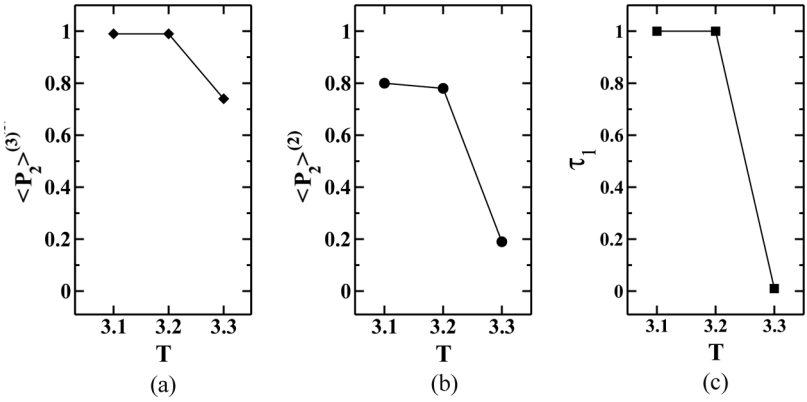

FIGURE 7 Temperature dependence of the order parameters: (a) $\langle P_2 \rangle^{(3)}$, (b) $\langle P_2 \rangle^{(2)}$ and (c) τ_1 for $k = 25$ and $\phi_0 = 140°$. Between temperatures $T = 3.2$ and 3.3 there is a phase transition from biaxial, antiferroelectric, hexagonal crystal into uniaxial nematic.

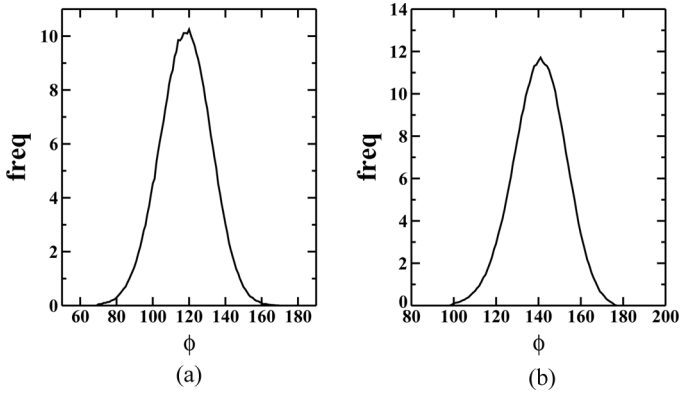

FIGURE 8 (a) Histogram of opening angles for $k = 25$ and $\phi_0 = 120°$; (b) histogram of opening angles for $k = 25$ and $\phi_0 = 140°$. In both cases $T = 3.3$.

For the last set of parameters chosen: $k = 25$ and $\phi_0 = 140°$ we found the same structures as for $k = \infty$ and $\phi_0 = 140°$, but with transition temperatures shifted to lower values (Fig. 7). Histogram of the opening angles in the nematic phase (Fig. 8(b)) is comparable with the case shown in Fig. 8(a).

Summarizing, the preliminary results presented indicate that the bent-core systems with fluctuating opening angle behave quite similar to their rigid counterparts. For the parameters studied we did not observe any new phases as compared to $k = \infty$ cases. The only effect found was the lowering of the transition temperatures.

REFERENCES

[1] Acharya, B. R., Primak, A., & Kumar, S. (2004). *Phys. Rev. Lett.*, *92*, 145506.
[2] Madsen, L. A., Dingemans, T. J., Nakata, M., & Samulski, E. T. (2004). *Phys. Rev. Lett.*, *92*, 145505.
[3] Kurosu, H., Kawasaki, M., Hirose, M., Yamada, M., Kang, S., Thisayukta, J., Sone, M., Takezoe, H., & Watanabe, J. (2004). *J. Phys. Chem.*, *108*, 4674.
[4] Takezoe, H. & Takanishi, Y. (2006). *Japanese Journal of Applied Physics*, *45*, 597.
[5] Memmer, R. (2002). *Liq. Cryst.*, *29*, 483.
[6] Lansac, Y., Maiti, P. K., Clark, N. A., & Glaser, M. A. (2003). *Phys. Rev. E*, *67*, 011703.
[7] Dewar, A. & Camp, P. J. (2004). *Phys. Rev. E*, *70*, 011704.
[8] Orlandi, S., Berardi, R., Stelzer, J., & Zannoni, C. (2006). *J. Chem.Phys.*, *124*, 124907.1.
[9] Gay, J. G. & Berne, B. J. (1981). *J. Chem. Phys.*, *74*, 3316.
[10] Allen, M. P. & Tildesly, D. J. (1987). *Computer Simulation of Liquids*, Clarendon: Oxford.